

Rotating Hele-Shaw cells with ferrofluids

José A. Miranda*

Laboratório de Física Teórica e Computacional, Departamento de Física, Universidade Federal de Pernambuco, Recife, PE 50670-901, Brazil

(Received 16 November 1999; revised manuscript received 14 February 2000)

We investigate the flow of two immiscible, viscous fluids in a rotating Hele-Shaw cell, when one of the fluids is a ferrofluid and an external magnetic field is applied. The interplay between centrifugal and magnetic forces in determining the instability of the fluid-fluid interface is analyzed. The linear stability analysis of the problem shows that a nonuniform, azimuthal magnetic field, applied tangential to the cell, tends to stabilize the interface. We verify that maximum growth rate selection of initial patterns is influenced by the applied field, which tends to decrease the number of interface ripples. We contrast these results with the situation in which a uniform magnetic field is applied normally to the plane defined by the rotating Hele-Shaw cell.

PACS number(s): 68.10.-m, 75.50.Mm, 75.70.Ak, 47.20.Ma

When a fluid is pushed by a less viscous one in a narrow space between two parallel plates (the so-called Hele-Shaw cell), the well-known Saffman-Taylor instability phenomenon arises [1], which takes the form of fingering [2]. Traditionally, experiments and theory focus on two basic Hele-Shaw flow geometries: (i) rectangular [1] and radial [3]. In rectangular geometry cells the less viscous fluid is pumped against the more viscous one along the direction of the flow. Meanwhile, in the radial geometry case, the less viscous fluid is injected to invade the more viscous one, through an inlet located on the top glass plate. In both geometries, the viscosity-driven instability leads to the formation of beautiful fingering patterns.

In recent years, the quest for new morphologies and richer dynamic behavior resulted in a number of modifications of the classic Saffman-Taylor setup [4]. An interesting variation of the traditional viscosity-driven fingering instability is the investigation of radial Hele-Shaw flows in the presence of centrifugal driving. The inclusion of centrifugal forces can be considered by rotating the cell, with constant angular velocity, around an axis perpendicular to the plane of the flow. In this case, the interface instability can be driven by the density difference between the fluids. In the late 1980s Schwartz [5] performed the linear stability analysis of the rotating cell problem, in the limits of high density and viscosity contrast. More recently, Carrillo *et al.* [6] studied, both theoretically and experimentally, flow in a rotating Hele-Shaw cell in arbitrary density and viscosity contrast. They extended the linear analysis performed in Ref. [5] by considering that the inner fluid is injected in the cell through a hole at the center of rotation, with constant injection rate. The linear growth rate calculated in Ref. [6] shows that the interface instability can be driven by both the density difference and the viscosity contrast between the fluids. Their experimental results supported their theoretical analysis. Carrillo and co-workers also examined the radial displacement of a rotating fluid annulus, bound by a second fluid, in stable [7] and unstable [8] regimes. In another interesting work, Magdaleno *et al.* [9] applied a conformal mapping technique

to argue that the effects of rotation can be used to prevent cusp singularities in zero surface tension Hele-Shaw flows.

Another stimulating modification of the traditional Saffman-Taylor problem in non-rotating Hele-Shaw cells considers the interface morphology when one of the fluids is a ferrofluid [10], and an external magnetic field is applied perpendicular to the cell plates. Ferrofluids, which are colloidal suspensions of microscopic permanent magnets, respond paramagnetically to applied fields. As a result of the ferrofluid interaction with the external field, the usual viscous fingering instability is supplemented by a magnetic fluid instability [10], resulting in a variety of new interfacial behaviors [11–16].

The richness of new behaviors introduced by both rotation and magnetic field into the traditional Saffman-Taylor problem, motivated us to analyze the situation in which these two effects are simultaneously present. In this work we perform the linear stability analysis for flow in a rotating Hele-Shaw cell, assuming that one of the fluids is a ferrofluid and that a magnetic field is applied. First, we consider the situation in which a *nonuniform*, azimuthal, in-plane field is applied. The competition between rotation and magnetic field is analyzed. We show the azimuthal magnetic field provides a mechanism for stabilizing the interface. This field induced, stabilizing mechanism is proposed, and proved to be effective for flow in rotating Hele-Shaw cells. Through the analysis of the maximum growth rate, we verify that the azimuthal magnetic field acts to decrease the number of interface ripples. Finally, we contrast these results with the destabilizing situation in which a *uniform* magnetic field is applied normally to the plane defined by the rotating Hele-Shaw cell.

Consider a Hele-Shaw cell of thickness b containing two immiscible, incompressible, viscous fluids (see Fig. 1). Denote the densities and viscosities of the inner and outer fluids, respectively, as ρ_1 , η_1 and ρ_2 , η_2 . The flows in fluids 1 and 2 are assumed to be irrotational. Between the two fluids there exists a surface tension σ . We assume that the inner fluid is the ferrofluid (magnetization \vec{M}), while the outer fluid is nonmagnetic. During the flow, the fluid-fluid interface has a perturbed shape described as $\mathcal{R} = R + \zeta(\theta, t)$, where θ represents the polar angle, and R is the radius of the initially unperturbed interface.

*Email address: jme@lftc.ufpe.br

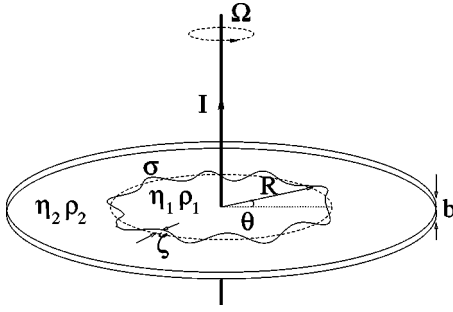


FIG. 1. Schematic configuration of the rotational Hele-Shaw flow with ferrofluid.

In order to include centrifugal forces, we allow the cell to rotate, with constant angular velocity Ω , about an axis perpendicular to the plane of the flow (Fig. 1). To include magnetic forces, we consider the action of an external magnetic field \vec{H} , produced by a long, straight wire carrying a current I , directed along the axis of rotation. By Ampere's law, it can be shown that the steady current I produces an azimuthal magnetic field external to the wire $\vec{H} = (I/2\pi r) \hat{\theta}$, where r is the distance from the wire, and $\hat{\theta}$ is the unit vector pointing in the direction of increase of θ .

Following the standard approximations used by Rosensweig [10] and others [11–13] we assume that the ferrofluid magnetization \vec{M} is collinear with the external field \vec{H} and that the influence of the demagnetizing field is neglected. It is also assumed that the ferrofluid is electrically nonconducting and that the displacement current is negligible. For the quasi-two-dimensional geometry of a Hele-Shaw cell, the three-dimensional flow may be replaced with an equivalent two-dimensional flow $\vec{v}(x, y)$ by averaging over the z direction perpendicular to the plane of the Hele-Shaw cell. Imposing no-slip boundary conditions and a parabolic velocity profile one derives Darcy's law for ferrofluids in a Hele-Shaw cell [13,17], which must be augmented by including centrifugal forces

$$\eta \vec{v} = -\frac{b^2}{12} \left\{ \vec{\nabla} p - \frac{1}{b} \int_{-b/2}^{+b/2} \mu_0 (\vec{M} \cdot \vec{\nabla}) \vec{H} dz - \rho \Omega^2 r \hat{r} \right\}, \quad (1)$$

where p is the hydrodynamic pressure, μ_0 is the free-space permeability, and \hat{r} denotes a unit vector pointing radially outward. Equation (1) describes nonmagnetic fluids by simply dropping the terms involving magnetization.

Since the velocity field \vec{v} is irrotational, it is convenient to rewrite Eq. (1) in terms of velocity potentials. We write $\vec{v} = -\vec{\nabla} \phi$, where ϕ defines the velocity potential. Similarly, we rewrite the magnetic body force in Eq. (1) as $\mu_0 (\vec{M} \cdot \vec{\nabla}) \vec{H} = \mu_0 M \vec{\nabla} H = \vec{\nabla} \Psi$, where we have introduced the scalar potential

$$\Psi = \mu_0 \int M(H) dH = \frac{\mu_0 \chi H^2}{2}, \quad (2)$$

with $M = M(H) = \chi H$, χ being a constant magnetic susceptibility.

With the definitions of ϕ and Ψ we notice that both sides of Eq. (1) are recognized as gradients of scalar fields. After integrating both sides of Eq. (1), we evaluate it for each of the fluids on the interface. Then, we subtract the resulting equations from each other, and divide by the sum of the two fluids' viscosities to get the equation of motion

$$\begin{aligned} A \left(\frac{\phi_2 + \phi_1}{2} \right) + \left(\frac{\phi_2 - \phi_1}{2} \right) \\ = -\frac{b^2}{12(\eta_1 + \eta_2)} \left\{ \sigma \kappa - \Psi + \frac{1}{2} (\rho_2 - \rho_1) \Omega^2 r^2 \right\}. \end{aligned} \quad (3)$$

To obtain Eq. (3) we have used the pressure boundary condition $p_1 - p_2 = \sigma \kappa$ at the interface, where $\kappa = \{ [r^2 + 2(\partial r / \partial \theta)^2 - r(\partial^2 r / \partial \theta^2)] / [r^2 + (\partial r / \partial \theta)^2]^{3/2} \}$ denotes the interfacial curvature in the plane of the Hele-Shaw cell. The dimensionless parameter $A = (\eta_2 - \eta_1) / (\eta_2 + \eta_1)$ is the viscosity contrast.

For the purpose of the following linear analysis, we perturb the interface with a single Fourier mode

$$\zeta(\theta, t) = \zeta_n(t) \exp(in\theta), \quad n = 0, 1, 2, \dots \quad (4)$$

The velocity potential for fluid j ($j = 1, 2$ indexes the inner and outer fluids, respectively), ϕ_j , obeys Laplace's equation $\nabla^2 \phi_j = 0$ and can be written as

$$\phi_j = \phi_j^0 + \phi_{jn} \left(\frac{R^n}{r^n} \right)^{(-1)^j} \exp(in\theta), \quad (5)$$

where ϕ_j^0 are independent of r and θ .

We need additional relations expressing the velocity potentials ϕ_j in terms of the perturbation amplitudes ζ , in order to conclude our derivation and close Eq. (3). To find these, we considered the kinematic boundary condition [10], which refers to the continuity of the normal velocity across the interface. Inserting expression (4) for $\zeta(\theta, t)$ and Eq. (5) for ϕ_j into the kinematic boundary condition, we solved for ϕ_{jn} consistently to first order in ζ to find

$$\phi_{jn} = (-1)^j \frac{R}{n} \dot{\zeta}_n, \quad (6)$$

where the overdot denotes total time derivative.

Substitute expression (6) for ϕ_{jn} into equation of motion (3), and again keep only linear terms in the perturbation amplitude. This procedure eliminates the velocity potentials from Eq. (3), and we obtain the differential equation for the perturbation amplitudes $\dot{\zeta}_n = \lambda(n) \zeta_n$, implying that the relaxation or growth of the mode n is proportional to the factor $\exp[\lambda(n)t]$, where

$$\lambda(n) = \frac{b^2 \sigma n}{12(\eta_1 + \eta_2) R^3} [N_\Omega - N_B - (n^2 - 1)] \quad (7)$$

is the linear growth rate. We define the dimensionless parameters $N_\Omega = [R^3(\rho_1 - \rho_2)\Omega^2] / \sigma$, and $N_B = \mu_0 \chi I^2 / (4\pi^2 \sigma R)$

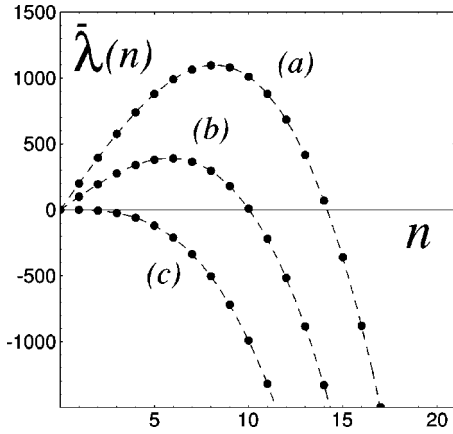


FIG. 2. Variation of the dimensionless growth rate $\bar{\lambda}(n) = [12(\eta_1 + \eta_2)R^3/b^2\sigma]\lambda(n)$ as a function of n for $N_\Omega = 200$ and (a) $N_B = 0$, (b) $N_B = 100$, and (c) $N_B = 200$. The peak location and width of the band of unstable modes decrease with increasing N_B .

as the rotational and magnetic bond numbers, respectively. N_Ω (N_B) measures the relative strength of centrifugal (magnetic) and capillary effects.

Inspecting Eq. (7) for the linear growth rate $\lambda(n)$ we observe the interplay of rotation, magnetic field and surface tension in determining the interface instability. If $\lambda(n) > 0$ the disturbance grows, indicating instability. As usual, the contribution coming from the surface tension term has a stabilizing nature (σ stabilizes modes of large n). The factor $(n^2 - 1)$ in Eq. (7) arises directly from the first order terms in ζ present in the curvature, while the overall factor of n can be traced to the fact that in the generalized Darcy's law (1) the velocity is proportional to gradients of an effective pressure. With these considerations in mind, let us focus on the relation between rotation and magnetic field. As a result of centrifugal forcing N_Ω may be either positive or negative, depending on the relative values of the fluid's densities. If the inner fluid is more dense ($\rho_1 > \rho_2$), $N_\Omega > 0$ and rotation plays a destabilizing role. The opposite effect arises when $\rho_1 < \rho_2$. On the other hand, the azimuthal magnetic field contribution N_B always tends to stabilize the interface. This indicates that the rotation-driven instability could be delayed or even prevented if a sufficiently strong nonuniform, azimuthal magnetic field is applied in the plane of the flow.

A physical explanation for the stabilizing role of the magnetic field can be given based on its symmetry properties and nonuniform character. Notice that such a field possesses a radial gradient. The magnetic field influence is manifested as the existence of a body force due to field nonuniformity. The field produces a force directed radially inward, that tends to move the ferrofluid toward the current-carrying wire (regions of higher magnetic field). This force opposes the centrifugal force and favors interface stabilization. This effect is similar to the gradient-field stabilization mechanism discussed by Rosensweig [10] for inviscid three dimensional fluid flow problems, and by Zahn and Rosensweig [18] for viscous, unconfined ferrofluids.

In order to illustrate the role of the magnetic effects in the linear stages of the interface evolution, we plot in Fig. 2 the dimensionless growth rate $\bar{\lambda}(n) = [12(\eta_1 + \eta_2)R^3/b^2\sigma]\lambda(n)$ as a function of the mode number n , taking $N_\Omega = 200$

and $N_B = 0, 100, 200$. As expected, for zero applied field ($N_B = 0$) the interface is unstable. If we increase the magnitude of the applied field ($N_B = 100$), even though we get a narrower band of unstable modes, the interface remains unstable. If we keep increasing the magnetic field intensity, $\bar{\lambda}(n)$ becomes negative for all $n > 1$, and the interface tends to stabilize. In Fig. 2 we see that for $N_B = 200$ the interface is stable, due to the action of the azimuthal magnetic field.

A relevant physical quantity can be extracted from the linear growth rate: the fastest growing mode n^* , given by the closest integer to the maximum of Eq. (7) with respect to n [defined by setting $d\lambda(n)/dn = 0$],

$$n_{\max} = \sqrt{\frac{1}{3}[1 + (N_\Omega - N_B)]}. \quad (8)$$

As discussed by Carrillo *et al.* [6] for the nonmagnetic, rotating case, n^* is strongly correlated to the number of ripples present in the early stages of pattern formation. With the help of their experiments, the authors in Ref. [6] compared the number of ripples with n^* and found a remarkable agreement. Taking this fact into account, and inspecting Eq. (8) we verify that, for positive N_Ω , an increasingly larger N_B does not only tend to decrease the finger growth rate, but also tends to decrease the number of interface ripples. The azimuthal magnetic field (or correspondingly, N_B) can be seen as a control parameter to discipline the number of interface undulations.

We conclude by contrasting the results obtained above (nonuniform, tangential field) with those which arise when a *uniform* external magnetic field is applied *perpendicular* to a rotating Hele-Shaw cell containing ferrofluid. By performing the linear stability analysis of the system, and using the closed form expressions for the magnetic term, recently derived in Ref. [14], we obtain the following linear growth rate:

$$\lambda^\perp(n) = \frac{b^2\sigma n}{12(\eta_1 + \eta_2)R^3} [N_\Omega + \mathcal{D}_n(p)N_B^\perp - (n^2 - 1)], \quad (9)$$

where

$$\mathcal{D}_n(p) = \frac{p^2}{2} \left\{ \left[\psi\left(n + \frac{1}{2}\right) - \psi\left(\frac{3}{2}\right) \right] + \left[\mathcal{Q}_{n-1/2}\left(\frac{p^2+2}{p^2}\right) - \mathcal{Q}_{1/2}\left(\frac{p^2+2}{p^2}\right) \right] \right\}, \quad (10)$$

$N_B^\perp = \mu_0 M^2 b / 2\pi\sigma$ is the magnetic bond number for the perpendicular field configuration, and $p = 2R/b$ is the aspect ratio. The aspect ratio p should not be confused with the pressure. \mathcal{Q}_n represents the Legendre function of the second kind, while the Euler's psi function ψ is the logarithmic derivative of the Gamma function [19]. Notice that the function $\mathcal{D}_n(p) \geq 0$ for $n > 0$. In contrast to the nonuniform, azimuthal applied field discussed earlier, a uniform, perpendicular magnetic field tends to destabilize the interface. If the interface is already unstable with respect to rotations ($N_\Omega > 0$), the introduction of the magnetic field increases the interface insta-

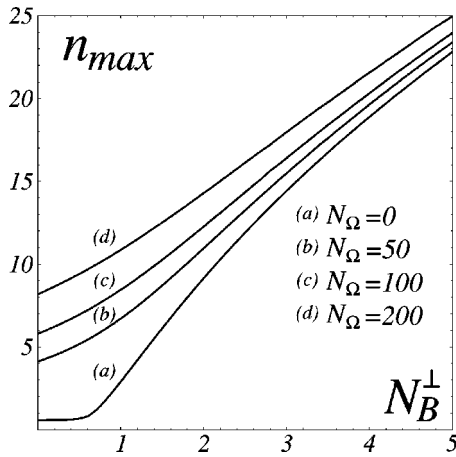


FIG. 3. Plot of n_{\max} as a function of N_B^\perp for increasing values of N_Ω , and $p=20$. These curves are obtained by numerically solving Eq. (11).

bility even further. On the other hand, if the outer fluid is more dense ($N_\Omega < 0$), the interface can still be deformed by the action of a perpendicular magnetic field.

By comparing the perpendicular field growth rate expression (9) with its azimuthal field counterpart (7), we notice that the presence of the function $\mathcal{D}_n(p)$ in Eq. (9) increases the complexity of the problem. Simple expressions for the

azimuthal case may become not so simple in the perpendicular field situation. Consider, for example, the calculation of the fastest growing mode n^* . In contrast to the simple expression for n_{\max} obtained in the azimuthal case [see Eq. (8)], the equivalent expression for the perpendicular configuration cannot be written in a simple form. It is now given by the solution of the transcendental equation

$$n^2 = \frac{1}{3} \left[1 + N_\Omega + \frac{\partial}{\partial n} [n \mathcal{D}_n(p)] N_B^\perp \right]. \quad (11)$$

Numerical evaluation of Eq. (11) shows that n_{\max} (and, consequently, n^*) increases with the magnitude of the perpendicular applied field. In this case, larger values of N_B^\perp tend to increase the number of interface ripples (see Fig. 3).

In summary, we have shown that the inclusion of magnetic effects into the rotating cell problem provides mechanisms for stabilizing/destabilizing the interface. Based on the relative simplicity of the experimental Hele-Shaw setup, it would be of considerable interest to perform experiments in Hele-Shaw cells simultaneously including centrifugal, magnetic, and injection driving. The combination of these effects is likely to lead to new and exciting interfacial patterns in the highly nonlinear regime.

This work was supported by CNPq and FINEP.

-
- [1] P. G. Saffman and G. I. Taylor, Proc. R. Soc. London, Ser. A **245**, 312 (1958).
 [2] For review articles on this subject, see D. Bensimon, L. P. Kadanoff, S. Liang, B. I. Shraiman, and C. Tang, Rev. Mod. Phys. **58**, 977 (1986); G. Homsy, Annu. Rev. Fluid Mech. **19**, 271 (1987).
 [3] L. Paterson, J. Fluid Mech. **113**, 513 (1981).
 [4] K. V. McCloud and J. V. Maher, Phys. Rep. **260**, 139 (1995).
 [5] L. W. Schwartz, Phys. Fluids A **1**, 167 (1989).
 [6] Ll. Carrillo, F. X. Magdaleno, J. Casademunt, and J. Ortín, Phys. Rev. E **54**, 6260 (1996).
 [7] Ll. Carrillo, J. Soriano, and J. Ortín, Phys. Fluids **11**, 778 (1999).
 [8] Ll. Carrillo, J. Soriano, and J. Ortín, Phys. Fluids **12**, 1685 (2000).
 [9] F. X. Magdaleno, A. Rocco, and J. Casademunt, e-print cond-mat/9910127 1999.
 [10] R. E. Rosensweig, *Ferrohydrodynamics* (Cambridge University Press, Cambridge, England, 1985), and references therein.
 [11] A. O. Tsebers and M. M. Maiorov, Magnetohydrodynamics **16**, 21 (1980).
 [12] S. A. Langer, R. E. Goldstein, and D. P. Jackson, Phys. Rev. A **46**, 4894 (1992).
 [13] D. P. Jackson, R. E. Goldstein, and A. O. Cebers, Phys. Rev. E **50**, 298 (1994).
 [14] J. A. Miranda and M. Widom, Phys. Rev. E **55**, 3758 (1997).
 [15] C. Flament, G. Pacitto, J.-C. Bacri, I. Drikis, and A. Cebers, Phys. Fluids **10**, 2464 (1998).
 [16] I. Drikis and A. Cebers, J. Magn. Magn. Mater. **201**, 339 (1999).
 [17] A. O. Tsebers, Magnetohydrodynamics **17**, 113 (1981).
 [18] M. Zahn and R. E. Rosensweig, J. Magn. Magn. Mater. **65**, 293 (1987).
 [19] I. S. Gradshteyn and I. M. Ryzhik, *Table of Integrals, Series, and Products* (Academic Press, New York, 1994).